



# Solar photodegradation of irinotecan in water: optimization and robustness studies by experimental design

Masho Hilawie Belay<sup>1,2</sup> · Federica Dal Bello<sup>3</sup> · Emilio Marengo<sup>1</sup> · Debora Fabbri<sup>4</sup> · Claudio Medana<sup>3</sup> · Elisa Robotti<sup>1</sup>

Received: 30 August 2022 / Accepted: 25 November 2022 / Published online: 7 December 2022  
© The Author(s), under exclusive licence to European Photochemistry Association, European Society for Photobiology 2022

## Abstract

Irinotecan, a widely prescribed anticancer drug, is an emerging contaminant of concern that has been detected in various aquatic environments due to ineffective removal by traditional wastewater treatment systems. Solar photodegradation is a viable approach that can effectively eradicate the drug from aqueous systems. In this study, we used the design of experiment (DOE) approach to explore the robustness of irinotecan photodegradation under simulated solar irradiation. A full factorial design, including a star design, was applied to study the effects of three parameters: initial concentration of irinotecan (1.0–9.0 mg/L), pH (5.0–9.0), and irradiance (450–750 W/m<sup>2</sup>). A high-performance liquid chromatography coupled with a high-resolution mass spectrometry (HPLC–HRMS) system was used to determine irinotecan and identify transformation products. The photodegradation of irinotecan followed a pseudo-first order kinetics. In the best-fitted linear model determined by the stepwise model fitting approach, pH was found to have about 100-fold greater effect than either irinotecan concentration or solar irradiance. Under optimal conditions (irradiance of 750 W/m<sup>2</sup>, 1.0 mg/L irinotecan concentration, and pH 9.0), more than 98% of irinotecan was degraded in 60 min. With respect to irradiance and irinotecan concentration, the degradation process was robust in the studied range, implying that it may be effectively applied in locations and/or seasons with solar irradiance as low as 450 W/m<sup>2</sup>. However, pH needs to be strictly controlled and kept between 7.0 and 9.0 to maintain the degradation process robust. Considerations about the behavior of degradation products were also drawn.

---

The last authorship is shared by Claudio Medana and Elisa Robotti.

---

✉ Federica Dal Bello  
federica.dalbello@unito.it

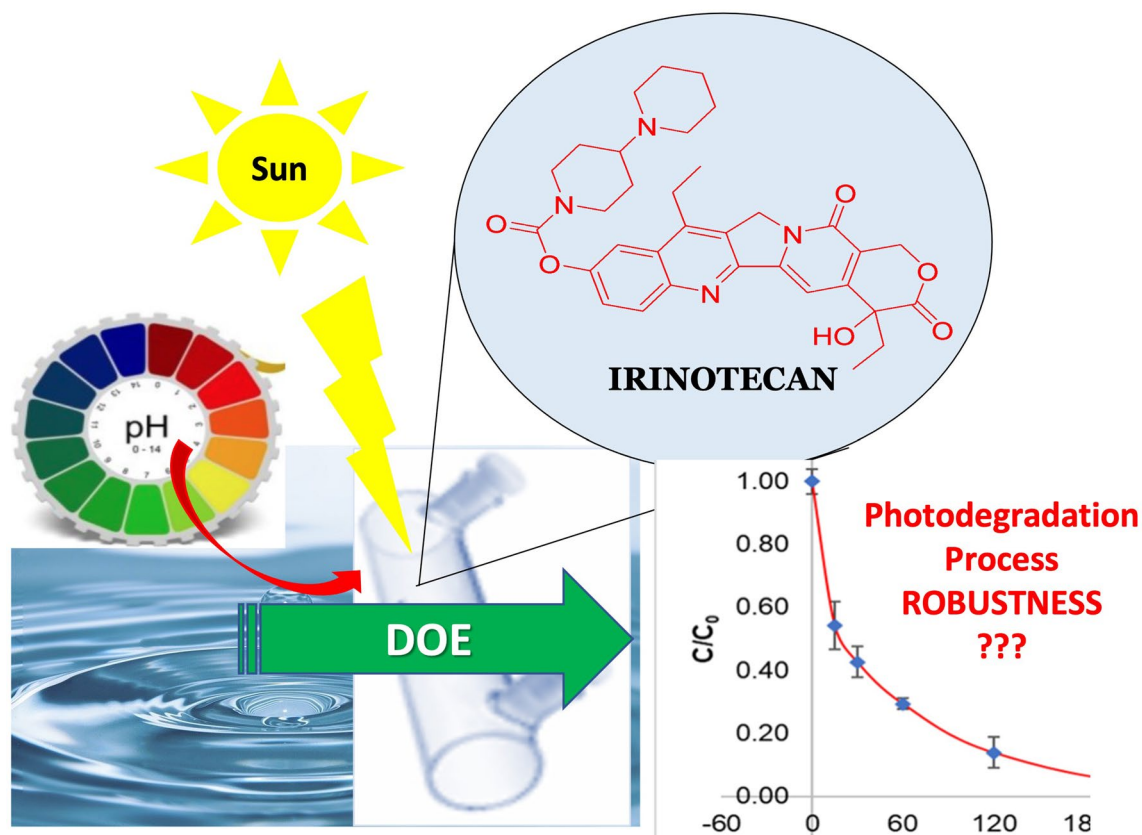
<sup>1</sup> Department of Sciences and Technological Innovation,  
University of Piemonte Orientale, Viale T. Michel 11,  
15121 Alessandria, Italy

<sup>2</sup> Department of Chemistry, College of Natural  
and Computational Sciences, Mekelle University,  
P. O. Box 231, Mekelle, Ethiopia

<sup>3</sup> Department of Molecular Biotechnology and Health  
Sciences, University of Turin, Via P. Giuria 5, 10125 Turin,  
Italy

<sup>4</sup> Department of Chemistry, University of Turin, Via P. Giuria  
5, 10125 Turin, Italy

## Graphical abstract



**Keywords** Emerging contaminants · Design of experiments · Irinotecan · Photodegradation · Robustness · Water

## 1 Introduction

There has been notable research and development in alternative wastewater treatment technologies over the last few decades to address new water treatment challenges such as inefficient removal of contaminants of emerging concern (CECs) in municipal wastewater treatment plants, rising demand for sustainable processes and technologies, and the circular economy [1, 2]. The presence of refractory and persistent CECs, such as pharmaceuticals and personal care products (PPCPs), is likely the most critical challenge, as these substances are harmful to aquatic organisms and human health [3]. As a result, various research projects have been initiated with the aim of developing more efficient treatment technologies. The AQUALITY project (<https://www.aquality-etn.eu/>), the framework within which the present work had been developed, is one of several interdisciplinary initiatives devoted to the development of different technologies to be used for the abatement of CECs, including advanced oxidation processes (AOPs) and nanofiltration (NF) technology [4].

The contaminant of emerging concern described in this study is irinotecan—an antineoplastic drug that is commonly used to treat colon and small cell lung cancers [5]. It was recently identified as one of the top 200 off-patent active substances in the European Union [6], indicating its widespread use. According to Slatter et al. [7], the human body excretes 45–63% of the administered irinotecan as parent drug, which normally enters the sewer system and eventually reaches surface water and groundwater. Irinotecan, like many other pharmaceuticals, has been detected in various environmental samples such as wastewater influents, effluents, and surface waters. For instance, Souza et al. [8] detected irinotecan in concentrations ranging between 1.21 and 2.03  $\mu\text{g/L}$  in 10 out of 14 hospital wastewater effluents in Brazil. The drug was also detected in several European wastewater effluents, ranging from 0.042 to 0.273  $\mu\text{g/L}$  in Spain [9–11], from 0.015 to 0.035  $\text{ng/mL}$  in Norway [12], and up to 49  $\text{ng/L}$  in Slovenia [13].

We previously identified eight transformation products (TPs) formed during the photodegradation of this drug [14], with the parent irinotecan molecule and one of its TPs being

detected in a hospital wastewater effluent. The TPs were formed in both ultrapure water (pH 4.3) and river water (pH 7.4) and were identified by low-resolution hybrid quadrupole ion trap (QTRAP) mass spectrometry system. Furthermore, Chatzimpaloglou et al. [15] identified 19 photolysis TPs of irinotecan at pH 7.0, including multiple isomers, using a high-pressure mercury lamp with a maximum wavelength of 365 nm. Unlike our prior work, Chatzimpaloglou and co-workers were able to identify multiple isomers using a combination of low-resolution triple quadrupole (LC-TQ) and high-resolution mass spectrometry (LC-TOF) and elucidated the structures of seven TPs. They showed in their study that formation of TPs initially increased the aquatic toxicity, measured using *Vibrio fischeri* bioassay, but subsequently declined by about threefold over the course of 2 h.

There is plenty of literature on the lab-scale successful application of AOPs for various aqueous matrices including surface water [14, 16, 17], produced water [18], wastewater [19, 20] and drinking water [21]. However, full-scale deployment of AOPs in water treatment plants is still challenging due to the complexity of the wastewater matrix and process and technological constraints [2]. The ultimate goal of the AQUALity project was to develop CECs' abatement strategies that are far more effective than conventional treatment technologies and to explore the possibility of applying the new methods in actual wastewater treatment plants (WWTPs). To that effect, it is necessary to define operational standards for a WWTP in terms of the parameters that may influence the degradation efficiency. This can be accomplished by the application of experimental design (DOE) methods [22] with the double purpose of optimizing the system and carrying out robustness studies to determine the effect of various parameters on the removal efficiency of the method under consideration.

Finding robustness means identifying an experimental region in which changing the values of the various operating parameters has no significant effect on the response of interest. Robustness studies, therefore, involve the use of the principles of DOE [22–24] to determine the effect of each experimental parameter (e.g., pollutant concentration and operating conditions) on the selected experimental response (e.g., residual CEC concentration and rate of degradation). Various studies in this field have demonstrated that the efficiency of AOPs in removing CECs is dependent on a variety of factors, including the CEC's properties (e.g., concentration and chemistry), the photocatalyst's properties (e.g., amount, size, structure, and doping), the aqueous solution's properties (e.g., pH and matrix components), and the reaction conditions (e.g., light intensity, temperature, and time) [25–29].

The present robustness study was designed to provide a guidance for operating WWTPs in the most efficient manner feasible (i.e., to maximize CECs' abatement) by

providing information on which parameters have no effect on the abatement efficiency or, on the contrary, which ones must be closely controlled. Plackett–Burman designs [30, 31] are the most widely used approaches in robustness studies. However, the application described in this paper used a combination of full factorial design and star designs [32]. This approach was chosen to allow for parallel optimization and robustness investigation while keeping the number of experiments to a minimum. Indeed, the employment of such experimental designs enables the evaluation of factor interactions and quadratic effects (these last ones, when the star design is included). The degradation studies must then be expressed in terms of abatement effectiveness: either by measuring the remaining concentration of the CEC or by calculating the rate of abatement as  $C/C_0$  (where  $C$  represents the concentration measured at a given time, and  $C_0$  is the initial concentration). To ensure the presence of a significant number of TPs, all experiments in the present applications were characterized for the concentration of the remaining CEC and, in some cases, for the peak areas of certain TPs, at a time greater than the half-time calculated at the center of the experimental domain. Thus, the experimental response was modeled using the surface response method in the studied experimental domain in order to build a model capable of explaining the effects of the factors involved, their interactions, and, ultimately, their quadratic effects. The generated model can provide the optimal operating conditions for the WWTP and information on the changes that should be made to the various parameters in the event of WWTP-related constraints (e.g., a fixed concentration of CEC and a constraint acting on the power of irradiation or the pH). The same model can be used to establish the robustness region of a certain WWTP, which provides guidance for process operation.

Despite the widespread occurrence and high persistence of irinotecan in the environment, as well as the formation of TPs with unknown effects, there are only limited studies on its presence in environmental samples, suggesting that this drug has received little attention. As a result, there are considerable gaps in our understanding of the drug's exposure levels, associated adverse effects, and environmental fate. Moreover, the lack of sensitive analytical methods for the accurate detection and quantification at extremely low concentrations of the drug and its TPs requires great attention. Therefore, it may be concluded that technologies capable of efficiently removing irinotecan from WWTPs are required in order to prevent or minimize its release into the environment. As briefly described above and in greater detail in our previous paper [14], direct photolysis via solar irradiation is a possible strategy for efficiently removing irinotecan from WWTPs. To ensure efficient photolysis, it is necessary to explore the effect of various parameters on the drug's photolytic degradation. In this paper, we report

the optimization and robustness investigation of irinotecan photolysis using experimental design (DOE) techniques. The information provided by this study can potentially be useful in real-world applications of the procedures considered for water and wastewater treatment. The parent molecule and its TPs were identified by HPLC coupled with an Orbitrap Mass Analyzer: details about method development are provided, together with the tentative identification of new TPs.

## 2 Materials and methods

### 2.1 Chemicals and reagents

Methanol (Ultra CHROMASOLV, > 99.9%), water (LC–MS grade), formic acid (98–100%), hydrochloric acid (HCl, 37%), sodium hydroxide ( $\geq 97\%$ , pellets), and irinotecan ( $\geq 97\%$ ) were purchased from Sigma-Aldrich (Milan, Italy). Acetonitrile (LC–MS grade) was from VWR (Milan, Italy). Stock standard solution of irinotecan was prepared in methanol at 1000 mg/L and used after proper dilutions for the HPLC–HRMS method development and optimization. The stock solution was stored at  $-20\text{ }^{\circ}\text{C}$  in amber glass vials in a dark standard-only freezer. For the photodegradation experiments, on the other hand, irinotecan aqueous solutions at the desired concentrations were always freshly prepared in ultrapure water.

### 2.2 Safety

To guarantee the best possible protection for personnel and the environment when working with irinotecan, all reagents must be handled with caution in accordance with the safety data sheet (SDS). In this study, all stock solutions were made in a biological safety hood with laminar airflow, and absorbent paper was used to protect the work surfaces. All disposable materials that came into touch with the substance under investigation were discarded as hazardous waste. Moreover, appropriate safety glasses, hand gloves, and lab coats were always worn to prevent chemical contamination and UV irradiation.

### 2.3 Experimental design

The robustness study involved three parameters: the intensity of the radiation ( $W$ ), the concentration of irinotecan (IRI), and the initial pH of the solution (pH). The levels adopted for each parameter are given in Table 1. The values for the center of the domain were chosen partly to provide measurable concentrations in HPLC–HRMS (e.g., irinotecan concentration) and partly as common values adopted in water treatment plants (e.g., the pH value is

**Table 1** Levels of each parameter adopted in the robustness study of irinotecan photolysis

Level	W ( $W/m^2$ )	IRI (mg/L)	pH
–1	450	1.0	5.0
0	600	5.0	7.0
1	750	9.0	9.0

**Table 2** DOE experiments performed for irinotecan photolysis

N <sup>o</sup>	W	IRI	pH	$C/C_0$	
1	–1	–1	–1	0.6554	Full factorial design ( $2^3$ )
2	1	–1	–1	0.7701	
3	–1	1	–1	0.5942	
4	1	1	–1	0.7418	
5	–1	–1	1	0.0311	
6	1	–1	1	0.0260	
7	–1	1	1	0.0190	
8	1	1	1	0.0330	
9	0	0	0	0.3500	Center points
10	0	0	0	0.3706	
11	0	0	0	0.3335	Star design
12	–1	0	0	0.2279	
13	1	0	0	0.2870	
14	0	–1	0	0.4804	
15	0	1	0	0.2457	
16	0	0	–1	0.6767	
17	0	0	1	0.0301	

usually quite close to neutrality). In line with this, the irradiance levels were selected based on values relevant to environmental applications, and the average irradiance in sunny days for low, medium, and high latitudes [33–36] was selected.

The three factors considered were studied by a two-level full factorial design, allowing the study of the main and their interaction effects, and a star design for the study of the main factors and their quadratic effects. Seventeen experiments were performed (Table 2), which included 8 (i.e.,  $2^3$ ) experiments of the full factorial design, 3 replications at the center of the domain and 6 experiments of the star design. In order to examine each experiment in terms of irinotecan disappearance ( $C/C_0$ ), the irinotecan concentrations before and after irradiation were determined using HPLC–HRMS. In addition, the signals of all TPs formed in each experiment were determined. Finally, DOE analyses were performed using Statistica software v. 7 (StatSoft Inc., Tulsa, OK, USA).

## 2.4 The irradiation procedure

Photodegradation experiments were carried out using simulated solar irradiation provided by a Solarbox 3000e (Cofomagra, Milan, Italy) equipped with a xenon lamp (2500 W) and a UV outdoor filter to better simulate the outdoor sunlight exposure by allowing > 290 nm wavelength to pass through. Microprocessor controllers were used to configure the test conditions such as irradiance and temperature of the irradiation system. Degradation experiments were performed using 14 mL Hellma 120-QS quartz glass cylindrical cuvettes with PTFE stoppers (Hellma GmbH, Jena, Germany), with a path length of 50 mm and diameter of 52.5 mm. The samples were irradiated at 20 cm distance from the light source. The pH values were adjusted using freshly prepared solutions of HCl and NaOH (0.01 N each), under pH-meter control.

Irinotecan solutions were prepared in ultrapure water at the concentrations and pH values predefined by the experimental design. An aliquot of the solution was taken before the degradation (sample  $t_0$ ), and irradiation in the solarbox took place under constant magnetic stirring using the programmed irradiance. After completion of each irradiation procedure, aliquots were withdrawn and immediately preserved in dark vials at  $-20\text{ }^\circ\text{C}$  until LC-HRMS analysis.

To understand the behavior of irinotecan photodegradation and select the appropriate time for the withdrawal of the sample during the irradiation, a preliminary kinetic study was conducted at the center of the experimental domain (i.e., irinotecan concentration of 5 mg/L, pH 7.0, and irradiance of  $600\text{ W/m}^2$ ). This allowed the determination of the degradation half-time in standard conditions. The irradiation periods considered were 0, 2, 4, 6, 8, 10, 15, 30, 60, 120, 240, and 480 min. The kinetic study allowed to identify the best sample withdrawal time for all the experiments of the DOE: this was fixed at 60 min of irradiation, a time close to the half-time calculated at the center of the domain (see Sect. 3) and also provided significant signals for most of the transformation products.

## 2.5 HPLC-HRMS analysis

The determination of irinotecan and the identification of its transformation products was performed using a Dionex Ultimate 3000 UHPLC system coupled with an Orbitrap Fusion Mass Spectrometer (Thermo Fisher, Massachusetts, USA), equipped with an electrospray ionization (ESI) source. The ESI source parameters, in positive ion mode, were as follows: spray voltage, 4000 V static; sheath gas, 35 arbitrary units; auxiliary gas, 21 arbitrary units; ion transfer tube temperature,  $300\text{ }^\circ\text{C}$ ; vaporizer temperature,  $275\text{ }^\circ\text{C}$ .

The chromatographic separation was achieved with a reversed-phase Luna C18(2) column ( $150\times 2.0\text{ mm}$ ,  $3\text{ }\mu\text{m}$ ; Phenomenex, Milan, Italy) using a mobile phase mixture of a 0.1% formic acid in water (A) and acetonitrile (B), set at a flow rate of 0.20 mL/min. The total run time was 48 min, and the gradient program was as follows: 0.0 min 5% B, 30.0 min 50% B, 34.0 min 100% B, 35.0 min 5% B, and 48.0 min 5% B. The column and autosampler temperatures were set at 40 and  $4\text{ }^\circ\text{C}$ , respectively. Injection volume was 20  $\mu\text{L}$ .

For each sample, two different acquisition modes have been performed: Full-scan MS (FS) and data-dependent MS<sup>2</sup> (ddMS<sup>2</sup>) scan. FS was performed in the range 100–800 m/z with  $R=60\text{ K}$ , and ddMS<sup>2</sup> acquisition mode using Collision-Induced Dissociation (CID, 20%) was a top 5 experiment where the 5 most abundant ions were fragmented in the range 100–800 m/z with  $R=30\text{ K}$ . All LC-HRMS data were processed using Xcalibur software [3.0.63].

## 2.6 Total organic carbon analysis

Total organic carbon (TOC) was measured using a Shimadzu (Milan, Italy) TOC-5000 analyzer through catalytic oxidation on Pt at  $680\text{ }^\circ\text{C}$ . The calibration was performed using potassium phthalate standards. TOC was evaluated at the optimal conditions for 0, 30, 60, and 120 min of irradiation.

## 3 Results and discussion

Irinotecan was detected at a retention time (RT) of 17.6 min with the protonated accurate mass value of  $m/z\ 587.2853$ , which was further confirmed by the well-defined isotopic pattern and fragmentation pathways as described in Sect. 3.3. Moreover, Fig. S1 (supplementary material) depicts the extracted ion chromatogram (EIC) of the irinotecan precursor ion.

### 3.1 Degradation kinetics and TOC analysis

To understand the behavior of irinotecan photodegradation in the conditions adopted in the present study, a preliminary kinetic study was conducted at the center of the experimental domain. This was necessary to determine the irinotecan degradation half-time ( $t_{1/2}$ ) in the conditions corresponding to the center of the domain. All the experiments of the DOE were, therefore, evaluated by withdrawing samples at a degradation time close to the half-time calculated at the center of the domain. The irradiation times considered were 0, 2, 4, 6, 8, 10, 15, 30, 60, 120, and 240 min. Figure 1 depicts the photodegradation of irinotecan with an embedded graph of the degradation rate and the 95% confidence limits. The degradation kinetics followed a pseudo-first order decay

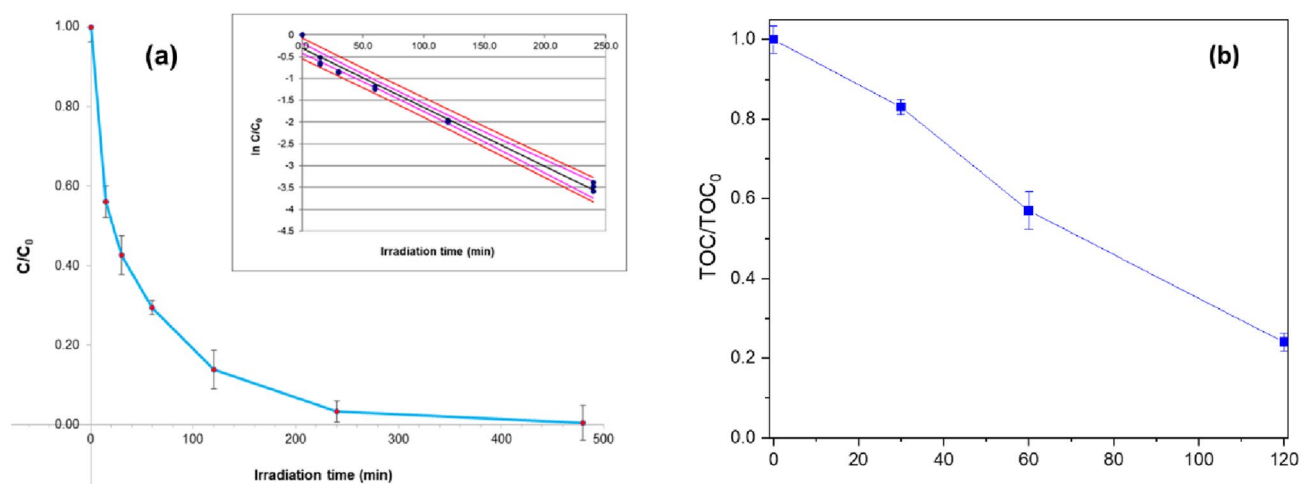


**Fig. 1** Irinotecan degradation kinetics (a) and the reduction of TOC (b)

fitting the line given by the following equation, where  $C_0$  represents the irinotecan initial concentration,  $C$  is the concentration at reaction time  $t$ , and  $k$  is the pseudo-first-order kinetic constant:

$$\ln(C) = -kt + \ln(C_0) \quad (1)$$

The  $R^2$  was equal to 0.9817 and the calculated half-time ( $t_{1/2}$ ) was 29.28 min with a kinetic rate constant of  $0.02411 \text{ min}^{-1}$ . Furthermore, most TPs had maximal abundance in the region between 30 and 60 min of irradiation (Fig. S2). As a result, the irradiation time for all the experiments of the DOE was set to 60 min to ensure both a time higher than the half-life under standard conditions and the presence of considerable amounts of the TPs. This allowed the investigation of the degradation process not only in terms of irinotecan disappearance rate, but also the formation of certain TPs.

TOC results obtained under optimal conditions revealed that a relatively small decline was initially observed due to the eventual formation of TPs in the first stage of the photo-transformation process. As the degradation progressed up to 2 h, TOC was significantly reduced. Moreover, the measured TOC agreed with a previous report on *Vibrio fischeri* toxicity [15], as well as the fact that not all TPs were completely degraded even after 2 h of irradiation.

### 3.2 Modeling the response C/C<sub>0</sub>

Each experiment of the DOE was carried out and aliquots of each sample were taken both at time  $t_0=0$  min and  $t_1=60$  min, which were then analyzed by HPLC-HRMS. For each experiment, the response  $C/C_0$  value was calculated from the concentration of irinotecan at  $t_0$  and  $t_1$ . After that,  $C/C_0$  was modeled

**Table 3** Sequential model fitting for the irinotecan photodegradation. The coefficients refer to coded values (in the range [-1; 1])

	t calc	p level	Coeff	Std. Err. Coeff
Intercept	21.24	<0.0001	0.345	0.016
pH	-15.56	<0.0001	-0.330	0.021

**Table 4** ANOVA results of the main parameters included in the final model

	SS	df	MS	F	p
pH	1.088	1	1.088	242.00	<0.0001
Error	0.067	15	0.004		
Total SS	1.156	16			

with respect to the three factors considered in this study. All the main factors, two-way interactions, and quadratic effects were included in the initial model (Fig. S3, a). The factors with no statistically significant effects (considering a significance level of  $\alpha=0.05$ ) were eliminated and the final model contained only the effect of pH (Fig. S3, b). Table 3 reports the coefficients (related to coded values) and  $t$  Student values calculated for the intercept and for pH, as well as the  $p$  levels and the errors of the coefficients. The calculated model resulted in a very good  $R^2$  value of 0.9416. The model adequacy was checked using ANOVA (Table 4).

The linear model calculated in terms of the coded values (-1, 0, and +1) is given by the following equation:

$$C/C_0 = 0.345 - 0.330 * pH \quad (2)$$

This mathematical equation represents the response factor given by the proportion of degradation of irinotecan after

60 min of solar photolysis. As evidenced by the concordance between observed and predicted responses, the model explained well the investigated experimental range. Furthermore, the residuals revealed no apparent trend (Fig. S4).

The model contained only the effect of pH; therefore, response surfaces are not needed to identify the best conditions; however, for a clearer discussion, the surface response of the interaction between pH and IRI is given in Fig. 2, calculated at an intermediate W level. The surface shows a huge effect of pH: increasing the pH leads to better results regardless of irinotecan concentration or irradiation intensity values. Irinotecan presents its strongest basic pKa value at 11.63 and its strongest acidic pKa at 9.17 (Fig. S13). Previous studies [14, 15] indicated that photolysis occurred very slowly in moderately acidic conditions. At pH 7, irinotecan appears almost entirely in one ionic form (a protonated tertiary amine group of the 1,4'-bipiperidine-1'-carbaldehyde), and as pH increases beyond 7, the neutral form is produced. At pH 9, the ratio of the two major species (protonated to neutral forms) is approximately 1:1. The rather fast kinetics observed along the pH range 7–9, in which irinotecan predominantly appears as neutral molecule, suggests that the neutral form of irinotecan is more prone to degradation. The effectiveness of degradation appears robust with respect to radiation intensity and the concentration of irinotecan since variations of these two parameters in the experimental domain investigated are not significant. For what regards pH, instead, the process appears not very robust. In most

situations, wastewaters have a pH value between 6.5 and 8.0 [23], which is also the optimal range for the majority of aquatic organisms, and many public and industrial treatment plants tend to operate as near to pH values around 7 (the center of the experimental domain) as possible. In these conditions  $C/C_0$  reaches values between 0.30 and 0.35 if the pH is maintained between 7.2 and 7.5. When pH increases, best degradation rates are obtained (between 0 and 0.15); nevertheless, in these conditions to have a good robustness of the final degradation, pH should be strictly controlled, if possible, above all if it shows more acidic values.

Changing the W value corresponds to carrying out solar degradation under different environmental conditions (i.e., sunny days for low, medium, or high latitudes). It is clear that natural solar irradiation conditions cannot be fixed by the operator, but these three levels have been applied during the experimentation. Fortunately, the model shows that the W value does not play a very significant role and the photolysis can be considered robust with respect to both the concentration of irinotecan and the W value. The same cannot be concluded for the pH value that should be controlled to guarantee a robust degradation procedure, above all if the pH values shift towards more acidic values. The best conditions for the overall process were identified by the model calculated (Eq. 2), as those giving the lowest possible calculated  $C/C_0$  value in the experimental domain investigated; these conditions involve a high pH value, while the other two parameters are not relevant (Table 5), and experiments

**Fig. 2** Response surface for the interaction between pH and IRI concentration at  $W=600 \text{ W/m}^2$  (central value)

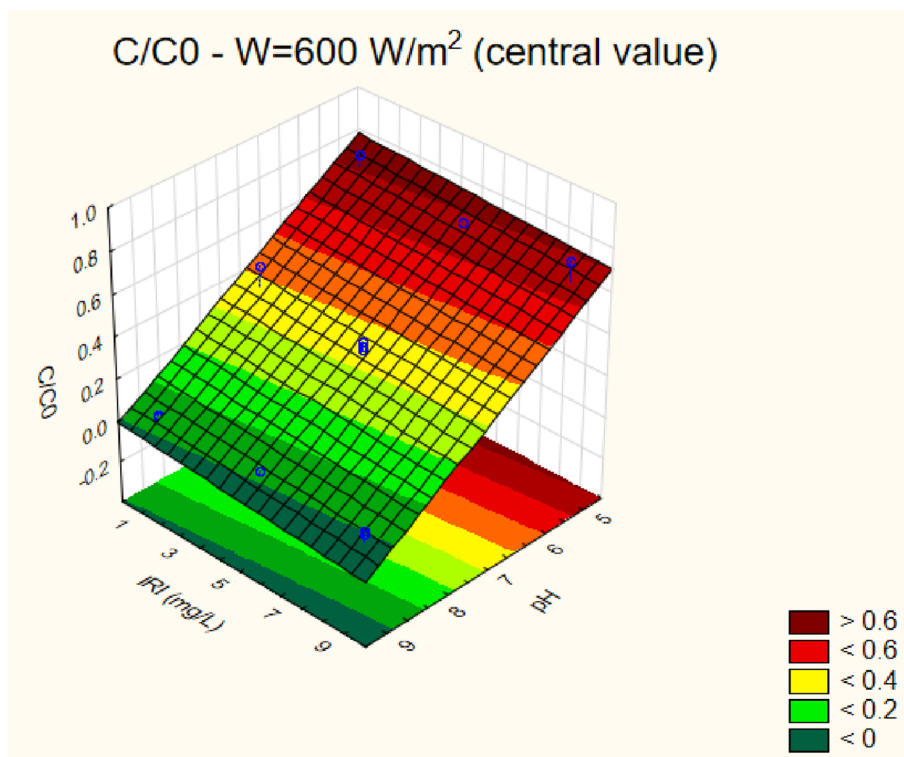


**Table 5** Best conditions obtained for the photodegradation of irinotecan. The table reports the conditions as actual values rather than as coded ones

Conditions	W	IRI	pH	Y pred	Y exp
Global optimum	/	/	9.0	0.015	0.019

performed at these conditions resulted in the removal of greater than 98% of irinotecan in 60 min of solar irradiation.

### 3.3 Identification of transformation products (TPs)

LC-HRMS in ESI positive ion mode was used to analyze all irinotecan samples. A total of 21 TPs, including multiple isomers, were detected as a result of the irinotecan photodegradation. Information such as  $m/z$  values, elemental compositions, retention times and product ions are reported in Table S1. The putative elemental composition of TPs was deduced by the means of Xcalibur software, based on mass accuracy (<5 ppm, without internal calibration) and ring double bond (RDB) index. Potential TPs on the basis of possible modifications reported in literature were searched [37] by providing known  $\Delta m/z$  differences. Thanks to the high mass resolution and accuracy of HRMS data, studies [38] have demonstrated that according to the guidelines suggested by Shymanski et al. [39], it is possible to tentatively elucidate unknown TPs at levels 3 and 2 or, when analytical standards are available, to identify them at level 1. In the present study, identification level 3 was assigned for seven TPs, in which tentative structures were elucidated by determining the most likely losses from the protonated molecules using the HRMS data collected from CID experiments.

The irinotecan structure has been divided into two major components (Fig. 3) to better explain fragmentation mechanisms and identification of TPs. Part A represents the 1,4'-bipiperidine-1'-carbaldehyde core, while Part B is the pyran-2-one moiety. In general, the transformations in the proposed structures took place in the pyran-2-one moiety (Part B), whereas the ions at  $m/z$  195,  $m/z$  167,  $m/z$  124, and  $m/z$  110 were all found at majority of the proposed TPs.

The protonated irinotecan molecular ion  $[M + H]^+$  with  $m/z$  587.2855 was detected at 17.63 min. Through collision-induced dissociation (CID) experiments, we investigated the fragmentation pathways and determined the most likely neutral losses from the protonated molecule. The MS/MS spectrum with the proposed fragmentation pathways is shown in Fig. S5. The proposed fragmentation pathways were agreed with those reported in previous works [14, 15].

Proposed structures for seven TPs are shown in Fig. 4. The mechanisms involved in the formation of these TPs have been described in detail in the supplementary material (Fig. S6-S11). TP-423 ( $m/z$  423.2393) and TP-439 ( $m/z$

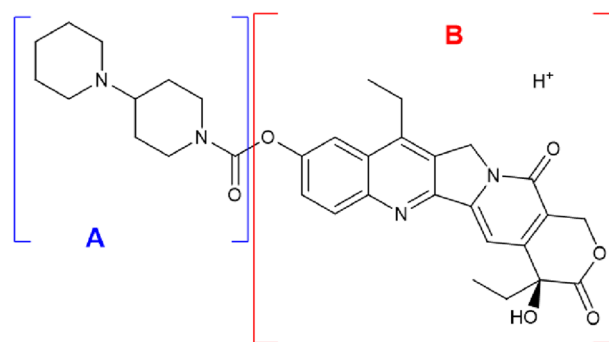


**Fig. 3** The protonated irinotecan molecule

439.2336), corresponding to the formulas  $C_{25}H_{35}N_4O_2^+$  and  $C_{26}H_{39}N_4O_2^+$ , had the smallest masses of all the detected TPs and their formation involved cleavage of the pyran-3,8-dione rings of irinotecan and opening of the cyclohexane-1,3-diene. Cleavage of the pyran-3,8-dione rings and oxidation of the pyrrolidine ring resulted in the formation of TP-573 ( $m/z$  573.2703) at 18.1 min, which corresponded to the formula  $C_{32}H_{37}N_4O_6^+$ . Two TPs with  $m/z$  561 were found at 15.6 min (TP-561a,  $m/z$  561.2346) and 17.1 min (TP-561b,  $m/z$  561.3075) due to cleavage of an acetylene group and a hydrogen rearrangement. In addition, hydroxylation of the parent irinotecan molecule resulted in the formation of three TPs, namely TP-603a, TP-603b, and TP-619. Monohydroxylation leads to two isomeric products with  $m/z$  603.2808 and  $m/z$  603.2811 identified at 17.0 and 18.4 min, respectively. TP-619 ( $m/z$  619.2741) was found at 15.5 min as a result of the dihydroxylation of irinotecan. The neutral losses from the 1,4'-bipiperidine-1'-carbaldehyde substructure were similar in irinotecan and the seven TPs, resulting in identical fragmentation pathways for  $m/z$  195, 167, 124, and 110.

### 3.4 Behavior of TPs in the experimental domain investigated

Since it was not possible to calculate the concentration of the TPs, their signals for each experiment were normalized for the corresponding  $C/C_0$  value. Then, models were built correlating the normalized signal of each TP to the process factors and their interactions. Very good results were obtained for two TPs (561a and 573), with  $R^2$  values equal to 0.9179 and 0.9235, respectively. Other TPs (611c, 593a and 439) reached  $R^2$  values of about 0.888, while 611b and 423 obtained  $R^2$  values of about 0.853. The obtained models are reported in Table 6, while the ANOVA results are reported in Table S2 (a-g). All the factors and interactions included in the models were significant at an  $\alpha$  value of 0.05. All the models contain W, pH and its squared effect, and the interaction between W and pH; the only exception was the



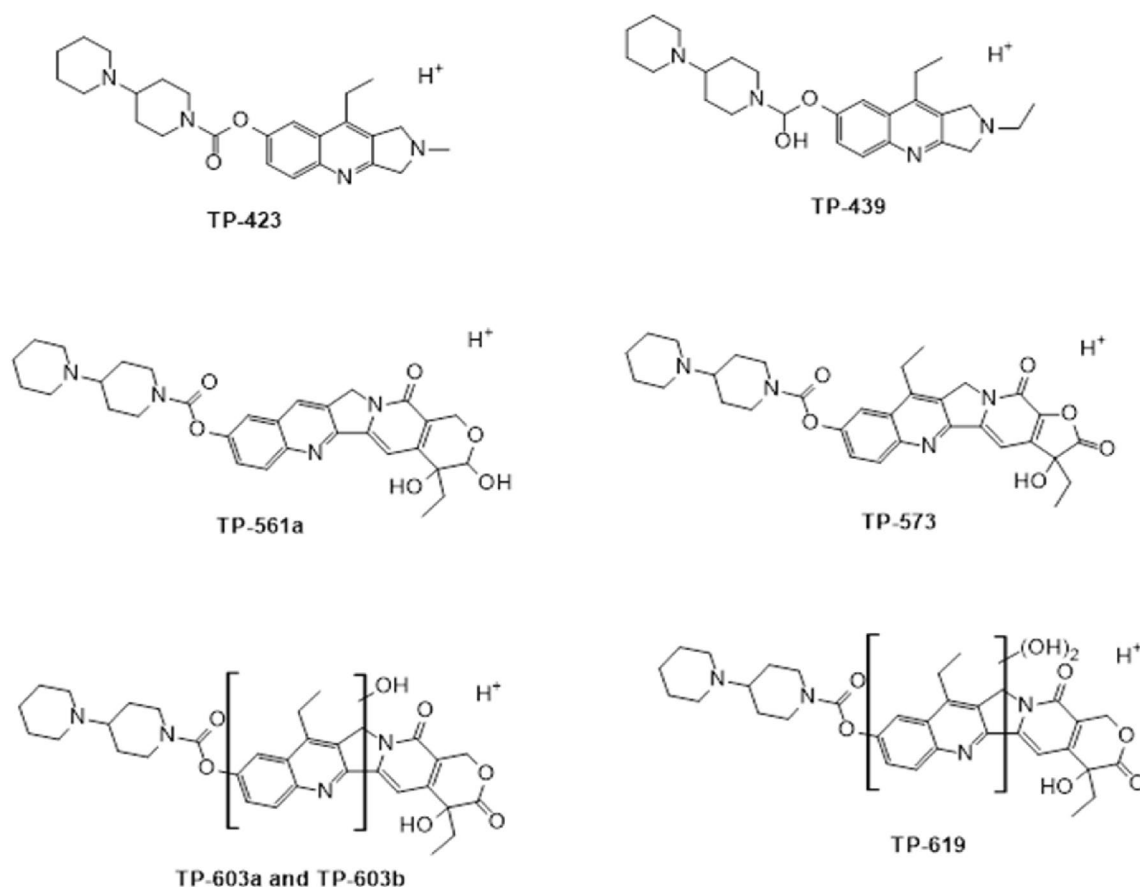


**Fig. 4** Proposed structures of seven irinotecan photodegradation TPs

model for TP-423 which just contained the effect of pH and its squared effect. The surface responses are reported in Fig. S12, showing the interaction between  $W$  and pH with [IRI] set at the central value.

Looking at the response surfaces (Fig. S12), the models report similar results: both at high and low  $W$  values, an increase of pH increases the signal of the TPs, but this increase is higher at high  $W$  values; at a low pH, the signal of TPs is low notwithstanding the value of  $W$ , while at high pH values, if  $W$  increases, the TPs signal increases. TP-423 shows a different behavior: the increase of pH increases the TP signal both at high and low  $W$  value and the  $W$  parameter does not play a relevant effect. The highest signal for the selected TPs is reached when  $W$  and pH are at the high levels, i.e., when the degradation of irinotecan is pushed to extremes. In terms of the modeled TPs and the contemporary presence of irinotecan, the robustness region corresponds to the center of the experimental domain. While a control of the pH is needed, the models appear more robust from the point of view of the  $W$  parameter. The region where irinotecan shows the best degradation rate is, of course, the region where the highest presence of TPs is detected; however, it should be noted that previous experimental evidence [15]

showed that the formation of degradation products resulted in increased aquatic toxicity in the first few minutes of the degradation process, but it was gradually reduced threefold in 2 h compared to the 60% initial inhibition reported for the parent irinotecan molecule.

## 4 Conclusions and forward

The robustness of irinotecan photodegradation in water was investigated by applying design of experiments on three factors (irinotecan concentration, pH, and solar irradiance). The photodegradation process followed a pseudo-first order kinetics with a half-time of 30 min. A total of 21 TPs were identified, among which tentative structures based on the HRMS data were elucidated for 7 TPs. The calculated model revealed that pH was the most important parameter affecting robustness (good robustness at pH 8–9). The maximum effect of pH and its squared effect were also generally revealed by models calculated for 7 TPs, with the response surfaces for irradiance found to be more robust, similar to that of irinotecan. Since the studied irradiance range corresponded to sunny days at low, middle, and high latitudes,

**Table 6** Models calculated for each TP: for each parameter included in the models, the value of the *t*-Student calculated, the *p*-level, the coefficient and its standard error are reported

TP-561a, $R^2=0.9179$	$t_{(1/2)}$	<i>p</i>	Coeff	Std. Err. Coeff
Intercept	1.717	0.1116	$6.5 \times 10^7$	$3.7 \times 10^7$
W	3.698	0.0030	$11.7 \times 10^7$	$3.2 \times 10^7$
pH	8.956	<0.0001	$28.3 \times 10^7$	$3.2 \times 10^7$
pH <sup>2</sup>	4.655	0.0006	$22.9 \times 10^7$	$4.9 \times 10^7$
W*pH	4.315	0.0010	$15.2 \times 10^7$	$3.6 \times 10^7$
TP-439, $R^2=0.8884$	$t_{(1/2)}$	<i>p</i>	Coeff	Std. Err. Coeff
Intercept	0.937	0.3671	$2.3 \times 10^7$	$2.5 \times 10^7$
W	4.309	0.0010	$9.0 \times 10^7$	$2.1 \times 10^7$
pH	6.336	<0.0001	$13.2 \times 10^7$	$2.1 \times 10^7$
pH <sup>2</sup>	3.575	0.0038	$11.6 \times 10^7$	$3.2 \times 10^7$
W*pH	4.905	0.0004	$11.4 \times 10^7$	$2.3 \times 10^7$
TP-593a, $R^2=0.8873$	$t_{(1/2)}$	<i>p</i>	Coeff	Std. Err. Coeff
Intercept	1.311	0.2145	$6.3 \times 10^6$	$4.8 \times 10^6$
W	3.853	0.0023	$15.4 \times 10^6$	$4.0 \times 10^6$
pH	6.869	<0.0001	$27.6 \times 10^6$	$4.0 \times 10^6$
pH <sup>2</sup>	3.521	0.0042	$22.0 \times 10^6$	$6.2 \times 10^6$
W*pH	4.473	0.0008	$20.0 \times 10^6$	$4.5 \times 10^6$
TP-423, $R^2=0.8538$	$t_{(1/2)}$	<i>p</i>	Coeff	Std. Err. Coeff
Intercept	1.143	0.2723	$2.4 \times 10^6$	$2.1 \times 10^6$
pH	7.798	<0.0001	$13.4 \times 10^6$	$1.7 \times 10^6$
pH <sup>2</sup>	4.577	0.0004	$12.3 \times 10^6$	$2.7 \times 10^6$
TP-573, $R^2=0.9235$	$t_{(1/2)}$	<i>p</i>	Coeff	Std. Err. Coeff
Intercept	1.584	0.1391	7.5E7	$4.7 \times 10^7$
W	4.344	0.0010	$17.3 \times 10^7$	$4.0 \times 10^7$
pH	8.827	<0.0001	$35.1 \times 10^7$	$4.0 \times 10^7$
pH <sup>2</sup>	4.953	0.0003	$30.7 \times 10^7$	$6.2 \times 10^7$
W*pH	4.859	0.0004	$21.6 \times 10^7$	$4.4 \times 10^7$
TP-611c, $R^2=0.8880$	$t_{(1/2)}$	<i>p</i>	Coeff	Std. Err. Coeff
Intercept	0.874	0.3994	$3.9 \times 10^6$	$4.5 \times 10^6$
W	4.220	0.0012	$15.8 \times 10^6$	$3.7 \times 10^6$
pH	6.431	<0.0001	$24.1 \times 10^6$	$3.7 \times 10^6$
pH <sup>2</sup>	3.506	0.0043	$20.5 \times 10^6$	$5.8 \times 10^6$
W*pH	4.866	0.0004	$20.4 \times 10^6$	$4.2 \times 10^6$
TP-611b, $R^2=0.8530$	$t_{(1/2)}$	<i>p</i>	Coeff	Std. Err. Coeff
Intercept	0.732	0.4779	$3.9 \times 10^6$	$5.3 \times 10^6$
W	3.556	0.0040	$15.6 \times 10^6$	$4.4 \times 10^6$
pH	5.548	0.0001	$24.4 \times 10^6$	$4.4 \times 10^6$
pH <sup>2</sup>	3.040	0.0103	$20.8 \times 10^6$	$6.9 \times 10^6$
W*pH	4.116	0.0014	$20.2 \times 10^6$	$4.9 \times 10^6$

and irradiance had no significant influence on robustness, it can be concluded that irinotecan degradation using solar irradiation may be applied in wastewater plants all over the world. The conditions corresponding to the highest

irinotecan degradation corresponded to the highest presence of these modeled TPs; however, the formation of TPs did not increase toxicity as shown by TOC reduction over time, agreeing with a previous bioassay study [15]. The findings

of this lab-scale study are encouraging and could be useful inputs for future efforts to integrate advanced oxidation processes into wastewater treatment processes. However, further research, for example on Pilot Plants, focusing on other operational parameters and wastewater matrix components, will be required.

**Supplementary Information** The online version contains supplementary material available at <https://doi.org/10.1007/s43630-022-00350-9>.

**Acknowledgements** This paper is part of a project that has received funding from the European Union's Horizon 2020 research and innovation program under the Marie Skłodowska-Curie Grant Agreement No 765860 (AQUALity).

**Author contributions** MHB: investigation, methodology, formal analysis, writing—original draft preparation, and writing—review and editing. FDB: data curation, formal analysis, and writing—review and editing. EM: conceptualization, software, writing—review and editing, and funding acquisition. DF: TOC analysis and writing—review and editing. CM: methodology, validation, writing—review and editing, and supervision. ER: conceptualization, software, writing—review and editing, supervision, and funding acquisition.

**Data availability** The data that support the findings of this study are available in the supporting information of this article.

## Declarations

**Conflict of interest** The authors declare no conflict of interest.

## References

- Golovko, O., Örn, S., Söregård, M., Frieberg, K., Nassazzi, W., Lai, F. Y., & Ahrens, L. (2021). Occurrence and removal of chemicals of emerging concern in wastewater treatment plants and their impact on receiving water systems. *Science of The Total Environment*, 754, 142122. <https://doi.org/10.1016/j.scitotenv.2020.142122>
- Iervolino, G., Zammit, I., Vaiano, V., & Rizzo, L. (2020). Limitations and prospects for wastewater treatment by UV and visible-light-active heterogeneous photocatalysis: a critical review. *Heterogeneous Photocatalysis*. [https://doi.org/10.1007/978-3-030-49492-6\\_7](https://doi.org/10.1007/978-3-030-49492-6_7)
- Papagiannaki, D., Morgillo, S., Bocina, G., Calza, P., & Binetti, R. (2021). Occurrence and human health risk assessment of pharmaceuticals and hormones in drinking water sources in the metropolitan area of Turin in Italy. *Toxics*, 9(4), 88. <https://doi.org/10.3390/toxics9040088>
- AQUALity (2017). Interdisciplinary cross-sectoral approach to effectively address the removal of contaminants of emerging concern from water (grant agreement ID: 765860). <https://cordis.europa.eu/project/id/765860>
- Besse, J. P., Latour, J. F., & Garric, J. (2012). Anticancer drugs in surface waters: what can we say about the occurrence and environmental significance of cytotoxic, cytostatic and endocrine therapy drugs? *Environment International*, 39(1), 73–86. <https://doi.org/10.1016/j.envint.2011.10.002>
- Wouters, O. J., Kanavos, P. G., & McKee, M. (2017). Comparing generic drug markets in Europe and the United States: Prices, volumes, and spending. *The Milbank Quarterly*, 95(3), 554–601. <https://doi.org/10.1111/1468-0009.12279>
- Slatter, J. G., Schaaf, L. J., Sams, J. P., Feenstra, K. L., Johnson, M. G., Bombardt, P. A., & Lord, R. S. (2000). Pharmacokinetics, metabolism, and excretion of irinotecan (CPT-11) following I.V. infusion of [<sup>14</sup>C] CPT-11 in cancer patients. *Drug Metabolism and Disposition*, 28(4), 423–433.
- Souza, D. M., Reichert, J. F., & Martins, A. F. (2018). A simultaneous determination of anti-cancer drugs in hospital effluent by DLLME HPLC-FLD, together with a risk assessment. *Chemosphere*, 201, 178–188. <https://doi.org/10.1016/j.chemosphere.2018.02.164>
- Gómez-Canela, C., Ventura, F., Caixach, J., & Lacorte, S. (2014). Occurrence of cytostatic compounds in hospital effluents and wastewaters, determined by liquid chromatography coupled to high-resolution mass spectrometry. *Analytical and Bioanalytical Chemistry*, 406(16), 3801–3814. <https://doi.org/10.1007/s00216-014-7805-9>
- Ferre-Aracil, J., Valcárcel, Y., Negreira, N., de Alda, M. L., Barceló, D., Cardona, S. C., & Navarro-Laboulais, J. (2016). Ozonation of hospital raw wastewaters for cytostatic compounds removal. Kinetic modelling and economic assessment of the process. *Science of The Total Environment*, 556, 70–79. <https://doi.org/10.1016/j.scitotenv.2016.02.202>
- Olalla, A., Negreira, N., de Alda, M. L., Barceló, D., & Valcárcel, Y. (2018). A case study to identify priority cytostatic contaminants in hospital effluents. *Chemosphere*, 190, 417–430. <https://doi.org/10.1016/j.chemosphere.2017.09.129>
- Schlabach M, Dye C, Kaj L, Klausen S, Langford K, Leknes H, Vogelsang C (2009) Environmental screening of selected organic compounds 2008. Human and hospital-use pharmaceuticals, aquaculture medicines and personal care products. *NILU OR*.
- Isidori, M., Lavorgna, M., Russo, C., Kundi, M., Žegura, B., Novak, M., & Heath, E. (2016). Chemical and toxicological characterisation of anticancer drugs in hospital and municipal wastewaters from Slovenia and Spain. *Environmental Pollution*, 219, 275–287. <https://doi.org/10.1016/j.envpol.2016.10.039>
- Gosetti, F., Belay, M. H., Marengo, E., & Robotti, E. (2020). Development and validation of a UHPLC-MS/MS method for the identification of irinotecan photodegradation products in water samples. *Environmental Pollution*, 256, 113370. <https://doi.org/10.1016/j.envpol.2019.113370>
- Chatzimpaloglou, A., Christophoridis, C., Fountoulakis, I., Antonopoulou, M., Vlastos, D., Bais, A., & Fytianos, K. (2021). Photolytic and photocatalytic degradation of antineoplastic drug irinotecan. Kinetic study, identification of transformation products and toxicity evaluation. *Chemical Engineering Journal*, 405, 126866. <https://doi.org/10.1016/j.cej.2020.126866>
- Brienza, M., Özkal, C. B., & Li Puma, G. (2018). Photo (Catalytic) oxidation processes for the removal of natural organic matter and contaminants of emerging concern from water. *Applications of Advanced Oxidation Processes (AOPs) in Drinking Water Treatment*. [https://doi.org/10.1007/978\\_2017\\_189](https://doi.org/10.1007/978_2017_189)
- Gonçalves, N. P., Iezzi, L., Belay, M. H., Dulio, V., Alygizakis, N., Dal Bello, F., & Calza, P. (2021). Elucidation of the photoinduced transformations of Aliskiren in river water using liquid chromatography high-resolution mass spectrometry. *Science of the Total Environment*, 800, 149547. <https://doi.org/10.1016/j.scitotenv.2021.149547>
- Jiménez, S., Andreozzi, M., Micó, M. M., Álvarez, M. G., & Contreras, S. (2019). Produced water treatment by advanced oxidation processes. *Science of the Total Environment*, 666, 12–21. <https://doi.org/10.1016/j.scitotenv.2019.02.128>

19. Deng, Y., & Zhao, R. (2015). Advanced oxidation processes (AOPs) in wastewater treatment. *Current Pollution Reports*, 1(3), 167–176. <https://doi.org/10.1007/s40726-015-0015-z>
20. Amor, C., Marchão, L., Lucas, M. S., & Peres, J. A. (2019). Application of advanced oxidation processes for the treatment of recalcitrant agro-industrial wastewater: a review. *Water*, 11(2), 205. <https://doi.org/10.3390/w11020205>
21. Polo-López, M. I., Nahim-Granados, S., & Fernández-Ibáñez, P. (2018). Homogeneous Fenton and photo-Fenton disinfection of surface and groundwater. *Applications of Advanced Oxidation Processes (AOPs) in Drinking Water Treatment*. [https://doi.org/10.1007/698\\_2017\\_129](https://doi.org/10.1007/698_2017_129)
22. Sakkas, V. A., Islam, M. A., Stalikas, C., & Albanis, T. A. (2010). Photocatalytic degradation using design of experiments: a review and example of the Congo red degradation. *Journal of Hazardous Materials*, 175(1–3), 33–44. <https://doi.org/10.1016/j.jhazmat.2009.10.050>
23. Ferreira, S. L., Caires, A. O., Borges, T. D. S., Lima, A. M., Silva, L. O., & dos Santos, W. N. (2017). Robustness evaluation in analytical methods optimized using experimental designs. *Microchemical Journal*, 131, 163–169. <https://doi.org/10.1016/j.microc.2016.12.004>
24. Barth, A. B., De Oliveira, G. B., Malesuik, M. D., Paim, C. S., & Volpato, N. M. (2011). Stability-indicating LC assay for butenafine hydrochloride in creams using an experimental design for robustness evaluation and photodegradation kinetics study. *Journal of Chromatographic Science*, 49(7), 512–518. <https://doi.org/10.1093/chrs/49.7.512>
25. Gnanaprakasam, A., Sivakumar, V. M., & Thirumarimurugan, M. (2015). Influencing parameters in the photocatalytic degradation of organic effluent via nanometal oxide catalyst: a review. *Indian Journal of Materials Science*. <https://doi.org/10.1155/2015/601827>
26. Gao, X., Guo, Q., Tang, G., Peng, W., Luo, Y., & He, D. (2019). Effects of inorganic ions on the photocatalytic degradation of carbamazepine. *Journal of Water Reuse and Desalination*, 9(3), 301–309. <https://doi.org/10.2166/wrd.2019.001>
27. Klavarioti, M., Mantzavinos, D., & Kassinos, D. (2009). Removal of residual pharmaceuticals from aqueous systems by advanced oxidation processes. *Environment International*, 35(2), 402–417. <https://doi.org/10.1016/j.envint.2008.07.009>
28. Ayodele, B. V., Alsaffar, M. A., Mustapa, S. I., & Vo, D. V. N. (2020). Backpropagation neural networks modelling of photocatalytic degradation of organic pollutants using TiO<sub>2</sub>-based photocatalysts. *Journal of Chemical Technology & Biotechnology*, 95(10), 2739–2749. <https://doi.org/10.1002/jctb.6407>
29. Tang, K., Casas, M. E., Ooi, G. T., Kaarsholm, K. M., Bester, K., & Andersen, H. R. (2017). Influence of humic acid addition on the degradation of pharmaceuticals by biofilms in effluent wastewater. *International Journal of Hygiene and Environmental Health*, 220(3), 604–610. <https://doi.org/10.1016/j.ijheh.2017.01.003>
30. Mašković, M., Jančić-Stojanović, B., Malenović, A., Ivanović, D., & Medenica, M. (2010). Assessment of liquid chromatographic method robustness by use of Plackett-Burman design. *Acta Chromatographica*, 22(2), 281–296. <https://doi.org/10.1556/achrom.22.2010.2.10>
31. Dejaegher, B., Dumarey, M., Capron, X., Bloomfield, M. S., & Vander Heyden, Y. (2007). Comparison of Plackett-Burman and supersaturated designs in robustness testing. *Analytica Chimica Acta*, 595(1–2), 59–71. <https://doi.org/10.1016/j.aca.2006.11.077>
32. Box, G. E., Hunter, W. H., & Hunter, S. (1978). *Statistics for experimenters* (Vol. 664). John Wiley and sons.
33. Katsoni, A., Gomes, H. T., Pastrana-Martínez, L. M., Faria, J. L., Figueiredo, J. L., Mantzavinos, D., & Silva, A. M. (2011). Degradation of trinitrophenol by sequential catalytic wet air oxidation and solar TiO<sub>2</sub> photocatalysis. *Chemical Engineering Journal*, 172(2–3), 634–640. <https://doi.org/10.1016/j.cej.2011.06.022>
34. Kuo, W. S., & Wu, C. L. (2012). Treatment of color filter wastewater by fresnel lens enhanced solar photo-Fenton process. *Advances in Materials Science and Engineering*. <https://doi.org/10.1155/2012/679206>
35. Weber, J., Halsall, C. J., Wargent, J. J., & Paul, N. D. (2009). A comparative study on the aqueous photodegradation of two organophosphorus pesticides under simulated and natural sunlight. *Journal of Environmental Monitoring*, 11(3), 654–659. <https://doi.org/10.1039/B811387D>
36. Fraser, T. R., Ross, K. E., Alexander, U., & Lenehan, C. E. (2022). Current knowledge of the degradation products of tattoo pigments by sunlight, laser irradiation and metabolism: a systematic review. *Journal of Exposure Science & Environmental Epidemiology*, 32(3), 343–355. <https://doi.org/10.1038/s41370-021-00364-y>
37. Kotthoff, L., O'Callaghan, S. L., Lisek, J., Schwerdtle, T., & Koch, M. (2020). Structural annotation of electro- and photochemically generated transformation products of moxidecin using high-resolution mass spectrometry. *Analytical and bioanalytical chemistry*, 412(13), 3141–3152. <https://doi.org/10.1007/s00216-020-02572-1>
38. Dal Bello, F., Mecarelli, E., Aigotti, R., Davoli, E., Calza, P., & Medana, C. (2022). Development and application of high resolution mass spectrometry analytical method to study and identify the photoinduced transformation products of environmental pollutants. *Journal of Environmental Management*, 308, 114573. <https://doi.org/10.1016/j.jenvman.2022.114573>
39. Schymanski, E. L., Jeon, J., Gulde, R., Fenner, K., Ruff, M., Singer, H. P., & Hollender, J. (2014). Identifying small molecules via high resolution mass spectrometry: communicating confidence. *Environmental Science and Technology*, 48(4), 2097–2098. <https://doi.org/10.1021/es5002105>

Springer Nature or its licensor (e.g. a society or other partner) holds exclusive rights to this article under a publishing agreement with the author(s) or other rightsholder(s); author self-archiving of the accepted manuscript version of this article is solely governed by the terms of such publishing agreement and applicable law.